




ORIGINAL ARTICLE

Enhanced mitochondrial activity reshapes a gut microbiota profile that delays NASH progression

María Juárez-Fernández^{1,2}  | Naroa Goikoetxea-Usandizaga³  | David Porras¹  |
 María Victoria García-Mediavilla^{1,2}  | Miren Bravo³  | Marina Serrano-Maciá³  |
 Jorge Simón^{2,3}  | Teresa C. Delgado³  | Sofía Lachiondo-Ortega³  |
 Susana Martínez-Flórez¹  | Óscar Lorenzo^{4,5}  | Mercedes Rincón⁶ |
 Marta Varela-Rey^{2,3} | Leticia Abecia^{7,8}  | Héctor Rodríguez⁷  | Juan Anguita^{7,9}  |
 Esther Nistal^{1,2}  | María Luz Martínez-Chantar^{2,3}  | Sonia Sánchez-Campos^{1,2} 

¹Institute of Biomedicine (IBIOMED), University of León, León, Spain

²Biomedical Research Network on Liver and Digestive Diseases (CIBERehd), Carlos III National Health Institute, Madrid, Spain

³Liver Disease Lab, Center for Cooperative Research in Biosciences (CIC bioGUNE), Basque Research and Technology Alliance (BRTA), Derio, Spain

⁴Laboratory of Diabetes and Vascular Pathology, IIS-Fundación Jiménez Díaz-Universidad Autónoma de Madrid, Madrid, Spain

⁵Biomedical Research Network on Diabetes and Related Metabolic Diseases-CIBERDEM, Madrid, Spain

⁶Department of Medicine, Immunobiology Division, University of Vermont, Burlington, Vermont, USA

⁷Inflammation and Macrophage Plasticity Laboratory, Center for Cooperative Research in Biosciences (CIC bioGUNE), Basque Research and Technology Alliance (BRTA), Derio, Spain

⁸Immunology, Microbiology and Parasitology Department, Medicine and Nursing Faculty, University of the Basque Country (UPV/EHU), Leioa, Spain

⁹IKERBASQUE, Basque Foundation for Science, Bilbao, Spain

Correspondence

María Luz Martínez-Chantar, CIC bioGUNE, Ed. 801A Parque Tecnológico de Bizkaia, 48160 Derio, Bizkaia, Spain.
 Email: mlmartinez@cicbiogune.es

Sonia Sánchez-Campos, Institute of Biomedicine, University of León, Campus de Vegazana, 24071 León, Spain.
 Email: ssanc@unileon.es

Funding information

Asociación Española contra el Cáncer; Ayudas Ramón y Cajal de la Agencia Estatal de Investigación, Grant/Award Number: RY2013-13666; BIOEF (Basque Foundation for Innovation and Health Research); Departamento de Industria del Gobierno Vasco; Fundación Científica de la Asociación Española Contra el Cáncer (AECC Scientific

Abstract

Background and Aims: Recent studies suggest that mitochondrial dysfunction promotes progression to NASH by aggravating the gut-liver status. However, the underlying mechanism remains unclear. Herein, we hypothesized that enhanced mitochondrial activity might reshape a specific microbiota signature that, when transferred to germ-free (GF) mice, could delay NASH progression.

Approach and Results: Wild-type and methylation-controlled J protein knockout (MCJ-KO) mice were fed for 6 weeks with either control or a choline-deficient, L-amino acid–defined, high-fat diet (CDA-HFD). One mouse of each group acted as a donor of cecal microbiota to GF mice, who

Abbreviations: BMI, body mass index; Ccr5, C-C chemokine receptor 5; CDA-HFD, choline-deficient, L-amino acid–defined, high-fat diet; CMT, cecal microbiota transplantation; Col1A1, collagen type 1 alpha 1 chain; dCDA-HFD/KO, MCJ-KO CDA-HFD–fed donor; Fatp2, fatty acid transport protein 2; GF, germ-free; MCJ, methylation-controlled J protein; MCJ-KO, methylation-controlled J protein knockout; mRNA, messenger RNA; NAD, nicotinamide adenine dinucleotide; NADH, reduced nicotinamide adenine dinucleotide; Nampt, nicotinamide phosphoribosyltransferase; Nlrp3, NOD, LRR- and pyrin domain-containing protein 3; OTU, operational taxonomic unit; PCA, principal component analysis; PCoA, principal coordinate analysis; SCFA, short-chain fatty acid; SIRT, sirtuin; Tgf-β, transforming growth factor beta; Tlr-4, Toll-like receptor-4; WT, wild type; ZO-1, zonula occludens 1.

María Juárez-Fernández and Naroa Goikoetxea-Usandizaga joint first authors.

This is an open access article under the terms of the [Creative Commons Attribution-NonCommercial-NoDerivs](https://creativecommons.org/licenses/by-nc-nd/4.0/) License, which permits use and distribution in any medium, provided the original work is properly cited, the use is non-commercial and no modifications or adaptations are made.

© 2022 The Authors. *Hepatology* published by Wiley Periodicals LLC on behalf of American Association for the Study of Liver Diseases.

Foundation) Rare Tumor Calls 2017; Instituto de Salud Carlos III, Proyectos de Investigación en Salud, Grant/Award Number: DTS20/00138; Junta de Castilla y León (FEDER), Grant/Award Number: GRS2126/A/2020, LE017P20 and LE063U16; Junta de Castilla y León cofunded by the European Social Fund; La Caixa Foundation Program; Ministerio de Ciencia e Innovación, Programa Retos-Colaboración, Grant/Award Number: RTC2019-007125-1; Ministerio de Ciencia, Innovación y Universidades, Grant/Award Number: FPU18/06257; Ministerio de Ciencia, Innovación y Universidades MICINN integrado en el Plan Estatal de Investigación Científica y Técnica y de Innovación, cofinanciado con Fondos FEDER, Grant/Award Number: PID2020-117116RB-I00; Ministerio de Economía y Competitividad/FEDER, Grant/Award Number: BFU2017-87960-R and PID2020-120363RB-I0; Proyecto Desarrollo Tecnológico CIBERehd

also underwent the CDA-HFD model for 3 weeks. Hepatic injury, intestinal barrier, gut microbiome, and the associated fecal metabolome were then studied. Following 6 weeks of CDA-HFD, the absence of methylation-controlled J protein, an inhibitor of mitochondrial complex I activity, reduced hepatic injury and improved gut-liver axis in an aggressive NASH dietary model. This effect was transferred to GF mice through cecal microbiota transplantation. We suggest that the specific microbiota profile of MCJ-KO, characterized by an increase in the fecal relative abundance of *Dorea* and *Oscillospira* genera and a reduction in *AF12*, *Alliboaaculum*, and [*Ruminococcus*], exerted protective actions through enhancing short-chain fatty acids, nicotinamide adenine dinucleotide (NAD⁺) metabolism, and sirtuin activity, subsequently increasing fatty acid oxidation in GF mice. Importantly, we identified *Dorea* genus as one of the main modulators of this microbiota-dependent protective phenotype.

Conclusions: Overall, we provide evidence for the relevance of mitochondria–microbiota interplay during NASH and that targeting it could be a valuable therapeutic approach.

INTRODUCTION

Mitochondrial dysfunction, together with oxidative stress and gut microbiota alteration, facilitates progression to NASH.^[1] In fact, it is known that the gut-liver axis is disrupted in NAFLD,^[2] although the specific microbiome signature associated with NAFLD and NASH has not been completely elucidated.^[3]

Recent studies have revealed a possible bidirectional interaction between mitochondrial dysfunction and gut microbiota.^[4] Dysregulation of mitochondrial functionality and the resulting increase in reactive oxygen species (ROS) may affect the gut microbiota by modulating the integrity of the intestinal barrier and thereby triggering the immune response. Oppositely, gut microbiota is known to regulate mitochondrial biogenesis, and microbial metabolites may also affect mitochondrial respiration.^[5] Therefore, targeting mitochondrial dysfunction could be the firewall to maintain a proper gut-liver axis, thereby delaying or even preventing NASH progression.

Methylation-controlled J protein (MCJ), or DnaJC15, is an endogenous negative regulator of the mitochondrial complex I.⁶ Its absence increases respiration and adenosine triphosphate (ATP) synthesis and stimulates the formation of respiratory supercomplexes, limiting the production of oxidative stress,^[6–8] as demonstrated in NASH.^[8–10] Besides, MCJ deficiency modifies the regulatory relationship between host mitochondria and gut microbiota during ulcerative colitis, affecting disease severity.^[11] Therefore, the *Mcj*-deficient mouse represents a reliable model to study the contribution of hepatic mitochondria to

gut dysbiosis and the altered gut-liver axis in NAFLD and NASH.

In this study, we aim to evaluate the effect of MCJ deficiency in a dietary mouse model of NASH, considering modifications of intestinal microbiota composition as a driving force, and to further determine if the hepatoprotective phenotype observed in methylation-controlled J protein knockout (MCJ-KO) mice could be transferred to germ-free (GF) mice through cecal microbiota transplantation (CMT).

METHODS

Experimental design

All procedures were performed in accordance with the ARRIVE guidelines and European Research Council guidelines for animal care and approved by CIC bioGUNE and University of León's institutional animal care and use committees (OEBA-ULE-003-2018 and CIC bioGUNE CBBA/IACUC [REGA 48/901/000/6106, P-CBG-CBBA-218]) followed by the competent authorities (Junta de Castilla y León and Diputación de Bizkaia, respectively). CIC bioGUNE is accredited by AAALAC Intl.

A Model: donor mice selection

Wild-type (WT) ($n = 14$) and MCJ-KO ($n = 19$) male mice aged 6 weeks with C57BL/6 background were housed at CIC bioGUNE animal facility. Animals were

fed a control diet or an L-amino acid with 60% kcal from fat, 0.1% methionine, and choline-deficient high-fat diet (CDA-HFD) (A06071302 Research Diets) for 6 weeks. Mice were then anesthetized with isoflurane 2.5% and euthanized by exsanguination using cardiac puncture. Cecal content was immediately preserved in skim milk (10%) with cysteine as reducing agent (0.5g/L), immersed in liquid nitrogen, and stored at -80°C until microbiota transplant. One mouse from each experimental group of Model A was selected as the gut microbiota donor based on the parameters specified in Table S1.

B Model: transplantation of gut microbiota

The 6-week-old GF male C57BL/6J mice ($n = 60$) were housed in a specific pathogen-free animal facility at the University of León. All mice were maintained under constant temperature, humidity, and light conditions and fed irradiated chow and autoclaved water ad libitum. After the acclimation period, the animals were transplanted with a single oral gastric gavage of 100 μl of the donor cecal content. Mice were divided into eight groups based on the four different types of donor transplanted microbiota and diet (Figure S1). After 3 weeks, all animals were euthanized by cardiac puncture under isoflurane anesthesia.

Sample collection

Liver, gut, brown adipose tissue and epididymal white adipose tissue (WAT), and fecal and cecal content of mice from Models A and B were collected, immediately immersed in liquid nitrogen, and stored at -80°C for posterior analysis. Blood was drawn and centrifuged at 6000 rpm for 10 min to obtain plasma.

RESULTS

Hepatic mitochondria improve intestinal barrier integrity and infer a particular gut microbiome signature in a lean-NASH mice model

Intestinal permeability was increased in WT mice after 6 weeks of CDA-HFD, shown by augmented serum fluorescein isothiocyanate (FITC)-dextran levels compared with control (Figure 1A). Interestingly, significantly decreased FITC-dextran permeability in CDA-HFD-fed MCJ-KO mice suggested a possible protective effect (Figure 1A). The histological evaluation presented no significant differences in ileum tissue on mucosal thickness, crypts depth, and villus height (Figure S3A).

Tight junction proteins analysis revealed significantly decreased messenger RNA (mRNA) levels of *Occludin* and *Zonula occludens 1* (*Zo-1*) (Figure 1B), claudin-1 positive immunostaining (Figure S3B), ZO-1 positive immunofluorescence (Figure 1C), and occludin protein levels (Figures 1D and S3C) in CDA-HFD-fed WT mice compared with both control and CDA-HFD-fed MCJ-KO mice, confirming improved junctional integrity in mice lacking MCJ, which may avoid bacterial and microbial product translocation.

The measurement of serum endotoxin and proinflammatory cytokines showed significantly reduced Lipid A plasma protein levels, a component of the lipopolysaccharide (Figures 1E and S3D), together with decreased proinflammatory IL-6 and TNF plasma concentration (Figure 1F) in CDA-HFD/KO group compared with WT.

Regarding gut-liver axis signaling, intestinal mRNA expression of *Farnesoid X receptor*, a nuclear bile acid receptor that regulates the secretion of antibacterial peptides, was increased in CDA-HFD-fed WT mice, compared with both control and CDA-HFD/KO group, and no changes were observed in *G Protein-Coupled Bile Acid Receptor-1* expression (Figure S3E). Besides, liver mRNA levels of *Toll-like receptor-4* (*Tlr-4*) and *NOD*, *LRR*-, and *pyrin domain-containing protein 3* (*Nlrp3*), sensors of gut microbiota-derived hepatotoxic or immunostimulatory compounds, were increased because of CDA-HFD intake; *Mcj* deficiency prevented *Nlrp3* upregulation (Figure 1G).

Altogether, MCJ deficiency counteracts the loss of intestinal barrier integrity, reduces the translocation of bacterial products, and modulates the inflammasome response in NASH.

Our group has previously demonstrated that the absence of MCJ ameliorates NAFLD.^[9] Because previous studies have described CDA-HFD as an aggressive model of lean NASH,^[12] we proceeded to analyze the role of MCJ in fatty liver disease under this diet. Firstly, liver histological analysis following CDA-HFD showed a high degree of microvesicular and macrovesicular steatosis, accompanied with inflammatory foci (Figure S2A). CDA-HFD also increased serum hepatic aminotransferase levels (Figure S2B). Importantly, both liver and WAT weight to body weight ratios were lower in CDA-HFD-fed MCJ-KO mice compared with WT (Figure S2C). Besides, lack of MCJ significantly reduced hepatic mRNA expression of the main proinflammatory cytokines, such as *C-C chemokine receptor 5* (*Ccr5*), *Il-1 β* , *Il-6*, and *Tnf* (Figure S2D). Regarding liver fibrosis, a significant reduction in the collagen content analyzed by Sirius Red stain (Figure S2E) and the expression of the profibrogenic *Collagen type 1 alpha 1 chain* (*Col1a1*) and *Transforming growth factor beta* (*Tgf- β*) in MCJ-KO mice also confirmed a remarkable deceleration in the development of fibrosis in the absence of MCJ (Figure S2F).

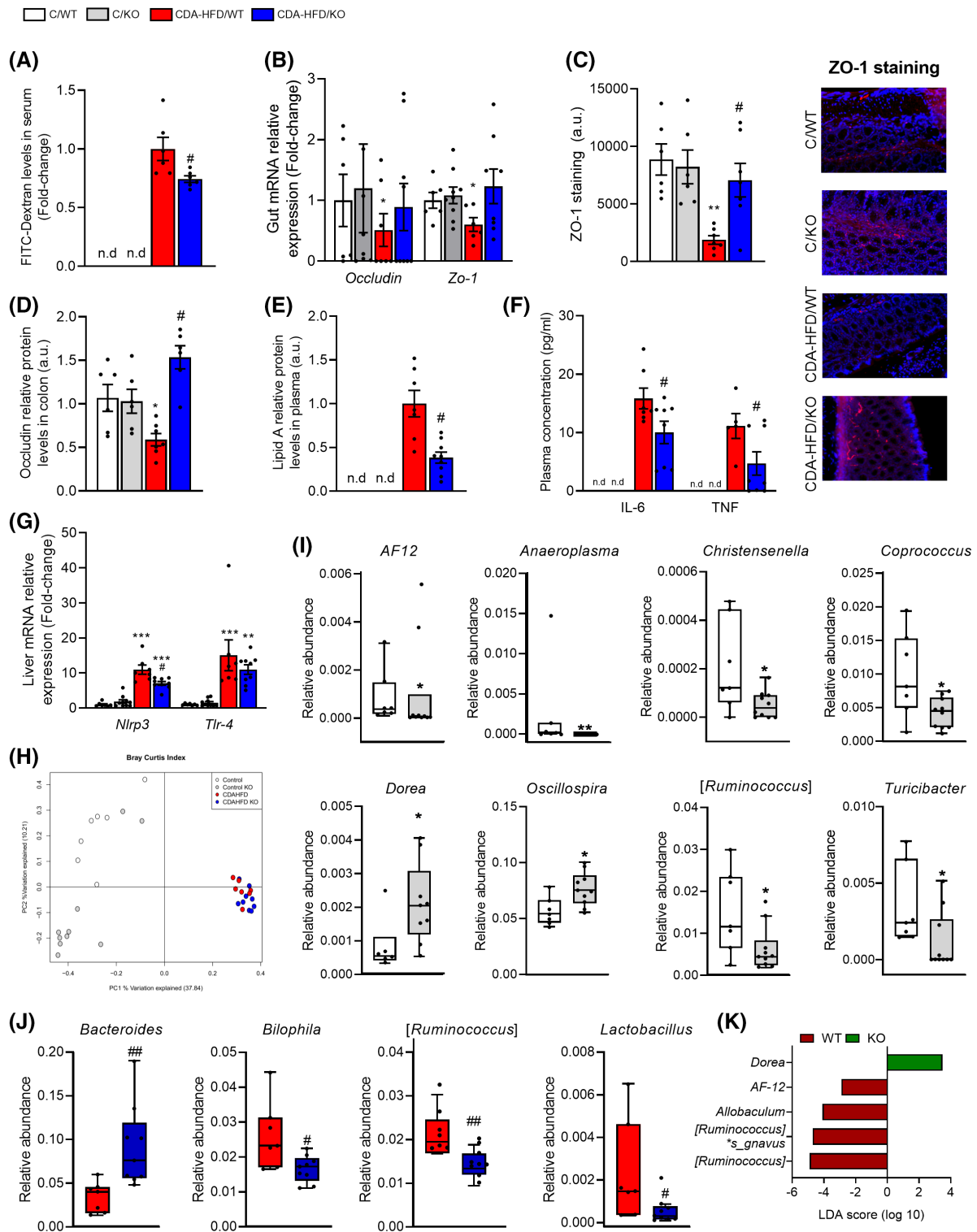


FIGURE 1 Effect of methylation-controlled J protein knockout (MCJ-KO) genotype on gut-liver axis and microbiota composition. (A) Fluorescein isothiocyanate (FITC)-dextran serum levels. (B) *Occludin* and *Zonula occludens 1 (Zo-1)* gut messenger RNA (mRNA) relative expression. (C) Quantification and representative ZO-1-stained ileum sections. (D) Densitometry analysis of *Occludin* levels in the ileum expressed as related to control-fed WT group (C/WT). (E) Densitometry analysis of Lipid A plasma levels expressed as related to choline-deficient, L-amino acid–defined, high-fat diet (CDA-HFD)/wild type (WT). (F) IL-6 and TNF plasma concentration. (G) *NOD*, *LRR*-, and *pyrin domain-containing protein 3 (Nlrp3)* and *Toll-like receptor-4 (Tlr-4)* hepatic mRNA relative expression. (H) Principal Coordinates Analysis plot based on Bray–Curtis' dissimilarity index at operational taxonomic unit (OTU) level. Differences in the relative abundance at genus level between WT and MCJ-KO mice fed with control (I) and CDA-HFD (J). (K) Linear discriminant analysis effect size at genus and species level of WT and MCJ-KO mice (threshold = 2.0 and $p < 0.05$). At least $n = 6$ were used in each experimental group. * $p < 0.05$, ** $p < 0.01$, *** $p < 0.001$ versus C/WT; # $p < 0.05$, ## $p < 0.01$ versus CDA-HFD/WT

The gut microbiome also determines NAFLD susceptibility.^[13] Therefore, fecal microbiota composition in A Model was analyzed.

A principal coordinate analysis (PCoA) based on Bray–Curtis index at operational taxonomic unit (OTU) level showed that the bacterial communities clustered separately along the first axis according to the diet ($F = 27.39$; $p < 0.0001$), whereas the second axis score plot suggested a possible cluster according to the genotype ($F = 1.99$; $p = 0.082$), mainly observed in the control diet–fed groups (Figure 1H).

After 3 weeks, CDA-HFD intake resulted in an increased microbiota diversity calculated by Shannon diversity index, whereas MCJ deficiency tended to decrease it (Figure S4A). The gut microbiota profile at phylum level was significantly modified because of diet and genotype (Figure S4B). Despite diet hugely modified gut microbiota composition also at the genus level, a specific profile was identified associated with the MCJ-KO genotype. The relative abundance of *AF12*, *Anaeroplasma*, *Christensenella*, *Coprococcus*, [*Ruminococcus*], and *Turicibacter* decreased in MCJ-KO group fed with control diet, whereas *Dorea* and *Oscillospira* showed an opposite pattern compared with WT mice (Figure 1I). Furthermore, changes associated with the MCJ-KO genotype depending on CDA-HFD feeding were also observed, pointing out an increase in *Bacteroides* genus and a reduction in *Bilophila*, *Lactobacillus*, and [*Ruminococcus*] (Figure 1J). Interestingly, some bacteria showed a genotype-dependent effect regardless of diet, that is, *Dorea* increased and *AF12*, *Allobaculum*, and [*Ruminococcus*] decreased in MCJ-deficient mice (Figure 1K). The differences at OTU level associated with MCJ-KO genotype were studied by linear discriminant analysis effect size analysis (Figure S4C).

This gut microbiota profile associated with MCJ-KO genotype on NASH development could play a key role in the hepatoprotective effect, avoiding fibrosis progression and preserving gut barrier integrity.

Gut microbiota transplantation from MCJ-KO mice to CDA-HFD–fed GF mice ameliorates hepatic injury

To study if the protective effects observed in CDA-HFD–fed MCJ-KO mice were due to a specific microbiome signature and, therefore, transferable, GF mice were subjected to CMT and fed CDA-HFD diet for 3 weeks (Figure S1). Individual values of the selected donors are depicted in Table S1.

CDA-HFD diet caused early NAFLD stages on transplanted GF mice, with increased hepatic steatosis, incipient inflammation, and ballooning, according to the histological evaluation (Figure 2A). Inflammation was attenuated in the MCJ-KO CDA-HFD–fed donor

(dCDA-HFD/KO) transplanted GF mice (Figure 2A). Besides, reduced hepatic triglycerides content (Figure 2B) and lower serum aminotransferase levels (Figure 2C) were also found in dCDA-HGF/KO transplanted mice compared with WT CDA-HFD–fed donor group. The study of proinflammatory cytokines confirmed these results, as expression of *Ccr5*, *Il-1 β* , *Il-6*, and *Tnf* was significantly downregulated following the CMT from MCJ-KO donors (Figure 2D). Moreover, in both MCJ-KO control diet–fed donor (dC/KO) and dCDA-HFD/KO receiver groups, fibrosis development was delayed, with significantly reduced alpha-smooth muscle actin staining (Figure 2E) and expression of *Col1a1*, *matrix metalloproteinase 9 (Mmp9)*, and *Tgf- β* (Figure 2F) compared with their WT microbiota transplanted counterparts.

Altogether, CDA-HFD–fed GF mice subjected to CMT from MCJ-KO donors showed reduced NASH progression. Thus, the hepatoprotective effect observed in MCJ-KO mice is transferable through gut microbiota transplantation.

MCJ-KO microbiota signature is transferable through CMT and preserves intestinal barrier integrity in CDA-HFD–fed GF mice

To determine the effect of CMT from MCJ-KO donors on gut barrier integrity and gut–liver axis, histological and gene expression studies were performed in GF mice fed with CDA-HFD. Ileum histological analysis showed no significant differences (Figure 3A). However, the relative expression of *Claudin-1* and *Zo-1* was increased in GF mice from MCJ-KO donors (Figure 3B), together with decreased liver mRNA levels of *Nlrp3* and *Tlr-4* (Figure 3C). Thus, the capacity of MCJ deficiency to counteract the upregulation of these genes, which was demonstrated in A Model, was also observed after CMT.

Venn diagrams were used to depict the transference of cecal microbiota at OTU level from each donor to every recipient group of GF mice. Around 50% of all OTUs were shared between every donor and both corresponding recipients, whereas others were shared at least with one of the receiver groups (Figure 3D). CDA-HFD–fed recipients showed a slightly decreased alpha diversity based on Shannon index compared with control-fed receivers, but this difference only reached significance for those groups transplanted with microbiota from WT donors (Figure S5A). Besides, PCoA based on the Bray–Curtis index at OTU level in GF mice fed with CDA-HFD revealed a clear separation of the cecal microbiota considering the donor's genotype according to the first axis ($F_{\text{donor genotype}} = 8.29$; $p < 0.0001$). However, the diet of the donors operated as another factor to

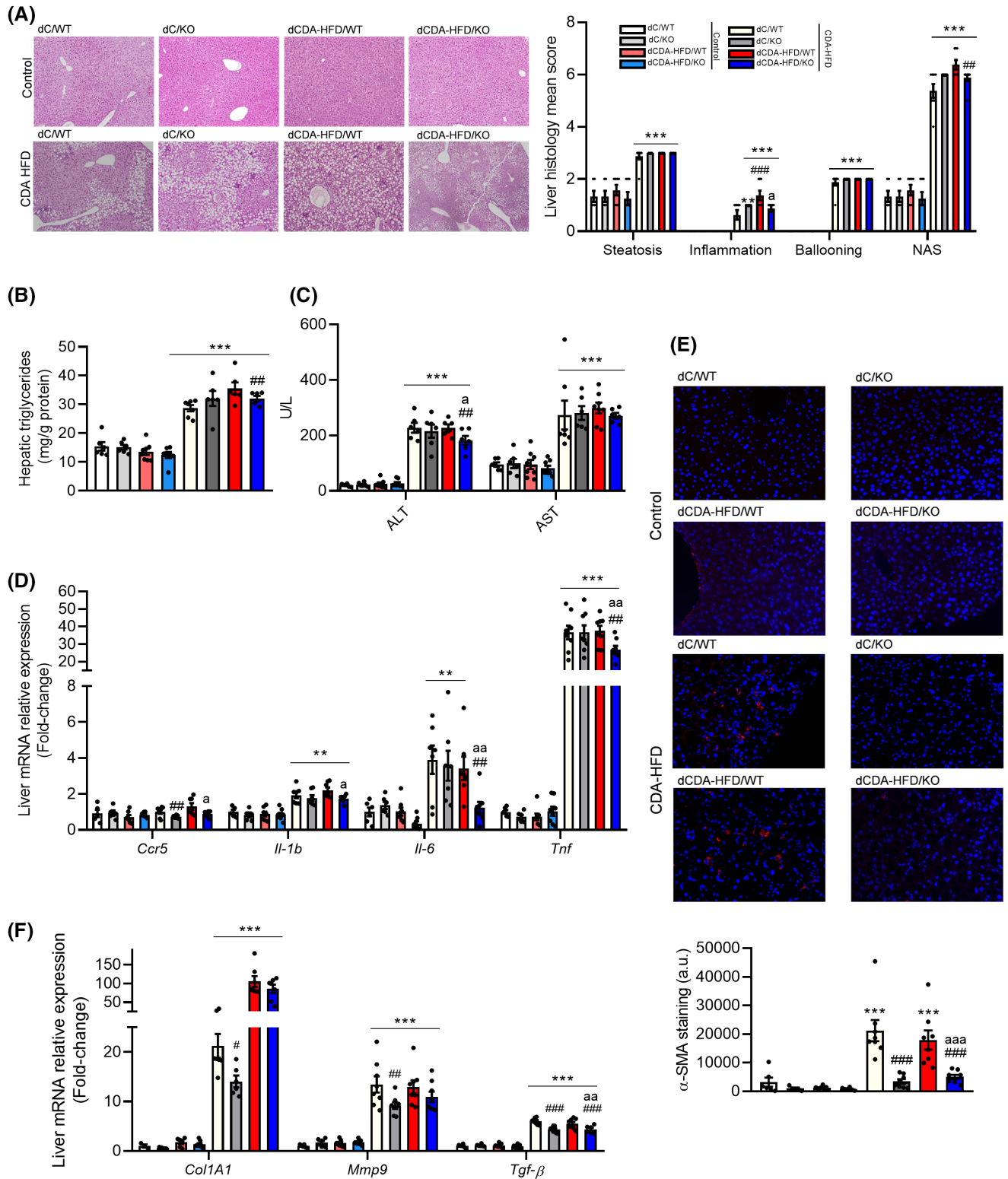


FIGURE 2 NAFLD-associated features development on transplanted germ-free mice from selected donors. (A) Hematoxylin and eosin-stained liver sections (×100) and NAFLD activity score (calculated from individual scores for steatosis, lobular inflammation, and ballooning). (B) Intrahepatic triglyceride content. (C) Alanine aminotransferase (ALT) and aspartate aminotransferase (AST) plasmatic levels. (D) Liver messenger RNA (mRNA) relative expression of inflammatory *C-C chemokine receptor 5 (Ccr5)*, *Il-1β*, *Il-6*, and *Tnf*. (E) Quantification and representative alpha-smooth muscle actin (α-SMA)-stained liver sections. (F) Liver mRNA relative expression of fibrosis markers *collagen type 1 alpha 1 chain (Col1a1)*, *matrix metalloproteinase 9 (Mmp9)*, and *transforming growth factor beta (Tgf-β)*. At least $n = 6$ were used in each experimental group. * $p < 0.05$, ** $p < 0.01$, *** $p < 0.001$ versus wild-type (WT) control diet-fed donor (dC/WT) (control diet); # $p < 0.05$, ## $p < 0.01$, ### $p < 0.001$ versus dC/WT (choline-deficient, L-amino acid-defined, high-fat diet [CDA-HFD]); ^a $p < 0.05$, ^{aa} $p < 0.01$, ^{aaa} $p < 0.001$ versus WT CDA-HFD-fed donor (dCDA-HFD/WT) (CDA-HFD)

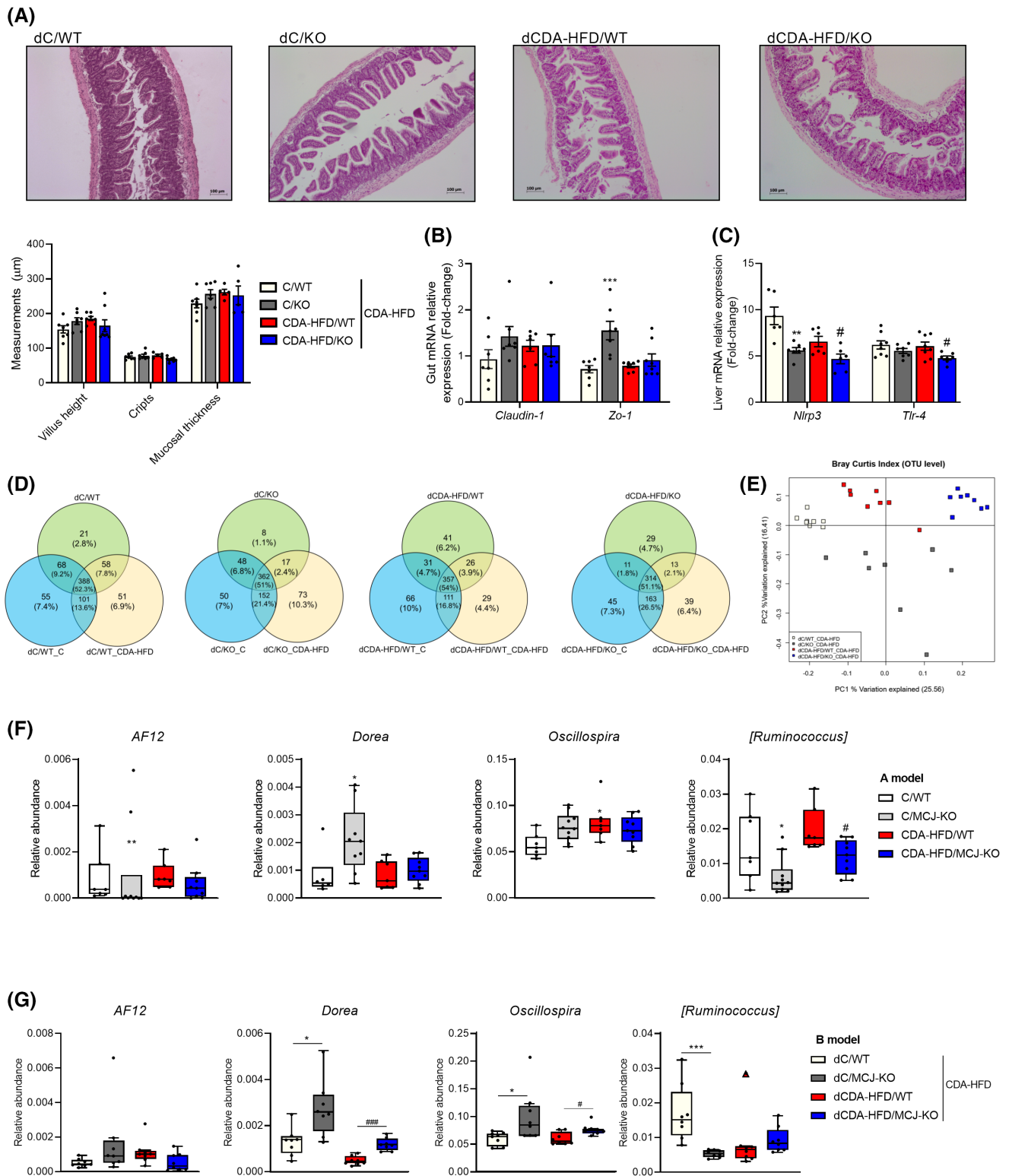


FIGURE 3 Effect of methylation-controlled J protein knockout (MCJ-KO) genotype transplantation in choline-deficient, L-amino acid–defined, high-fat diet (CDA-HFD)–fed germ-free (GF) mice on gut–liver axis and gut microbiota composition. (A) Hematoxylin and eosin–stained gut sections ($\times 100$), histological evaluation. (B) *Claudin-1* and *Zonula occludens 1* (*Zo-1*) gut messenger RNA (mRNA) relative expression. (C) *NOD*, *LRR*–, and *pyrin domain-containing protein 3* (*Nlrp3*) and *Toll-like receptor-4* (*Tlr-4*) hepatic mRNA relative expression. (D) Venn diagrams at operational taxonomic unit (OTU) level (relative abundance $>0.01\%$) from each donor to each recipient group of GF mice. (E) Principal coordinates analysis plot derived from Bray–Curtis dissimilarity index at OTU level of CDA-HFD–fed GF mice. Differences in the relative abundance at genus level in A Model (F) and in CDA-HFD–fed germ-free mice (B Model) (G). At least $n = 7$ were used in each experimental group. * $p < 0.05$, ** $p < 0.01$, *** $p < 0.001$ versus wild-type (WT) control diet–fed donor (dC/WT) (CDA-HFD); # $p < 0.05$, ### $p < 0.001$ versus WT CDA-HFD–fed donor (dCDA-HFD/WT) (CDA-HFD)

discriminate bacterial communities ($F_{\text{donor diet}} = 7.44$; $p < 0.0001$) (Figure 3E). Additionally, a PCoA based on Bray–Curtis index comparing all experimental groups was also performed (Figure S5B).

Microbiota composition analysis at phylum level in transplanted GF mice was influenced either by the diet or by donor's diet and genotype (Figure S5C). As in A Model, diet and genotype induced widespread changes in the gut microbial community structure at the phylum level (Figure S4C). At the genus level, the intestinal microbiota profile associated with MCJ-KO genotype (Figure 3F) was transferred through CMT to GF mice fed with CDA-HFD (Figure 3G). In A Model, the relative abundance of *AF12* and [*Ruminococcus*] showed a decreased pattern with the MCJ-KO genotype, whereas *Dorea* and *Oscillospira* showed an opposite trend (Figure 3F). The same gut microbiota profile was observed in the relative abundance of those genera in GF mice fed with CDA-HFD (Figure 3G) and control diet (Figure S5D).

Lack of MCJ increases hepatic NAD⁺ availability which is transferable through CMT, enabling augmented fatty acid oxidation

MCJ deficiency enhances lipid beta oxidation, ameliorating hepatic steatosis in diet-induced NAFLD models.^[9] Thus, we aimed to confirm the same effects in MCJ-KO mice (A Model). CDA-HFD-fed MCJ-KO mice showed significantly increased hepatic expression of *Fatty acid transport protein 2 (Fatp2)* and *Acyl-CoA dehydrogenase long chain (Acadl)* (Figure 4A), pointing out an enhanced lipid beta oxidation activity. Moreover, the availability of nicotinamide adenine dinucleotide (NAD⁺) is essential for fatty acid oxidation, since a heavily increased ratio of reduced nicotinamide adenine dinucleotide (NADH) to oxidized (NAD⁺) nicotinamide dinucleotide favors its inhibition. Analysis of the enzymes that take part in the NAD metabolism showed an increase in hepatic *Nicotinamide phosphoribosyltransferase (Nampt)* and *Sirtuin (Sirt) 1* relative expressions in CDA-HFD MCJ-KO mice compared with WT (Figure 4B). Interestingly, the measurement of hepatic NAD⁺, NADH, and their ratio exhibited a significantly increased NAD⁺ availability in CDA-HFD-fed MCJ-KO mice (Figure 4C).

We then aimed to study whether this increased NAD⁺ availability had also been transferred through CMT to GF mice fed with CDA-HFD. Hepatic expression of *Nampt* and *Sirt1* was significantly higher in GF mice receiving MCJ-KO microbiota (Figure 4D), along with significantly increased NAD⁺ availability (Figure 4E). Therefore, we measured the fatty acid oxidation activity and the expression of *Fatp2* and *Acadl* in the liver, confirming significantly increased activity in those GF mice subjected to MCJ-KO microbiota transplantation (Figure 4F,G).

To identify possible insights about the specific mechanisms by which the MCJ-KO metagenome exerts its hepatoprotective effect, correlation analyses were performed based on hepatic, metagenomic, and metabolomic results. Interestingly, in A Model, positive correlations between the relative abundance of *Dorea* genus and hepatic (1) NAD⁺/NADH ratio and (2) *Sirt1* expression were observed (Figure 4H,I). Besides, hepatic *Sirt1* and *Nampt* expression levels were also positively correlated with the relative abundance of *Dorea* in B Model (Figure 4J).

Therefore, increased availability of NAD⁺ found in the liver of MCJ-KO mice is transferable through CMT, enabling increased hepatic fatty acid oxidation and reduced NAS score and intrahepatic lipid accumulation.

The specific microbiome signature of MCJ-KO mice, linked with a concrete metabolome profile, favors intestinal NAD⁺ biosynthesis

After confirming the common microbiome signature between both models, we analyzed their fecal metabolome to identify possible mechanisms in which the gut microbiota is exerting this hepatoprotective effect.

In A Model, a principal component analysis (PCA) revealed a clear separation of metabolites according to the diet based on the first axis (38.6%) as well as a slight separation that was due to genotype (12%) (Figure 5A). Moreover, partial least square discriminant analysis was employed to identify metabolites discriminating WT and MCJ-KO mice that had been fed with control (Figure S6A) and CDA-HFD (Figure S6B), showing a certain metabolite profile associated with MCJ deficiency. The contribution of specific metabolites to each group was denoted by the Variables Importance in Projection (VIP) scores, showing the top 15 metabolites with higher VIP scores in animals fed with control diet (Figure S6C) and with CDA-HFD (Figure S6D). Although some metabolites that were allowed to discriminate between MCJ-KO and WT genotype were different between control and CDA-HFD-fed animals, others like riboflavin, isovalerylcarnitine, hexose, and indole were shared. The metabolites that were significantly related to MCJ deficiency independently of the diet were cytidine and riboflavin, whereas others like adenosine, carnitine, gentisic acid, or hydoxycholeate were also modified by genotype without reaching significance (Figure 5B). Additionally, MCJ deficiency in control-fed mice was associated with a significant decrease in deoxycholic acid and a significant increase in allantoin, carnosine, desthiobiotin, and sorbitol (Figure 5C). However, MCJ deficiency in CDA-HFD-fed mice did not report any significant differences in the detected metabolites, although a slight increase in betaine, bicine, and N-acetylneuraminic acid was observed,

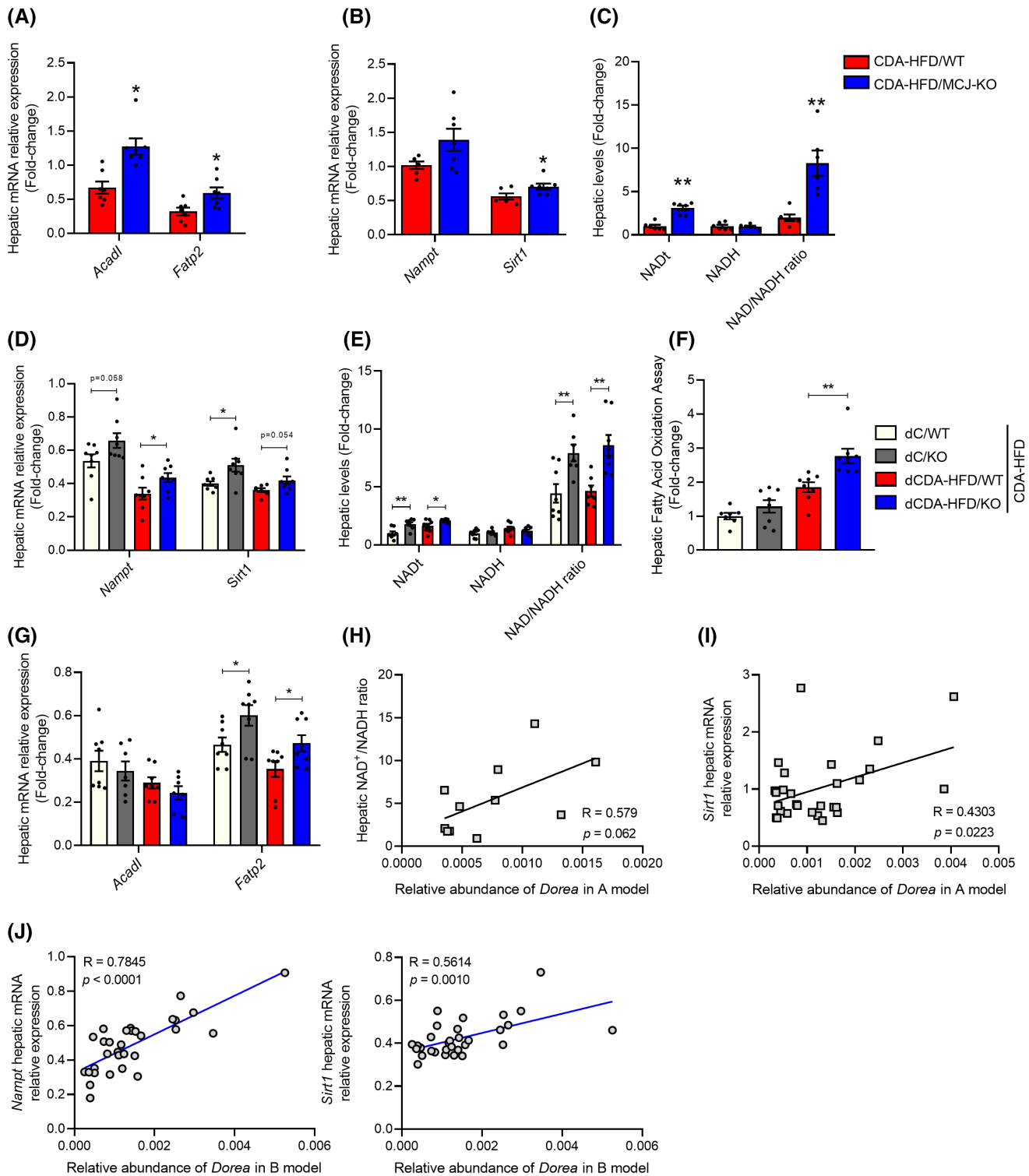


FIGURE 4 Hepatic fatty acid oxidation and nicotinamide adenine dinucleotide (NAD⁺) production in both A and B Models. A Model: (A) Liver messenger RNA (mRNA) relative expression of *Acadl* and fatty acid transport protein 2 (*Fatp2*). (B) Liver mRNA relative expression of NAD⁺ synthesis enzymes nicotinamide phosphoribosyltransferase (*Nampt*) and *Sirtuin* (*Sirt*) 1. (C) Hepatic levels of total NAD (NADt), reduced nicotinamide adenine dinucleotide (NADH), and NAD⁺/NADH ratio. B Model: (D) Liver mRNA relative expression of NAD⁺ synthesis enzymes *Nampt* and *Sirt1*. (E) Hepatic levels of NADt, NADH, and NAD⁺/NADH ratio. (F) Fatty acid oxidation assay. (G) Liver mRNA relative expression of *Acadl* and *Fatp2*. At least $n = 6$ were used in each experimental group. * $p < 0.05$; ** $p < 0.01$ versus choline-deficient, L-amino acid–defined, high-fat diet (CDA-HFD)/wild type (WT). Pearson's correlation coefficients, p values, and linear relationships between the relative abundance of *Dorea* and (H) the hepatic NAD⁺/NADH ratio and (I) the relative mRNA expression of *Sirt1* in A Model (black line and squares). (J) Pearson's correlation coefficients, p values, and linear relationships between the relative abundance of *Dorea* and the hepatic relative mRNA expression of *Nampt* and *Sirt1* in B Model (blue line and dots)

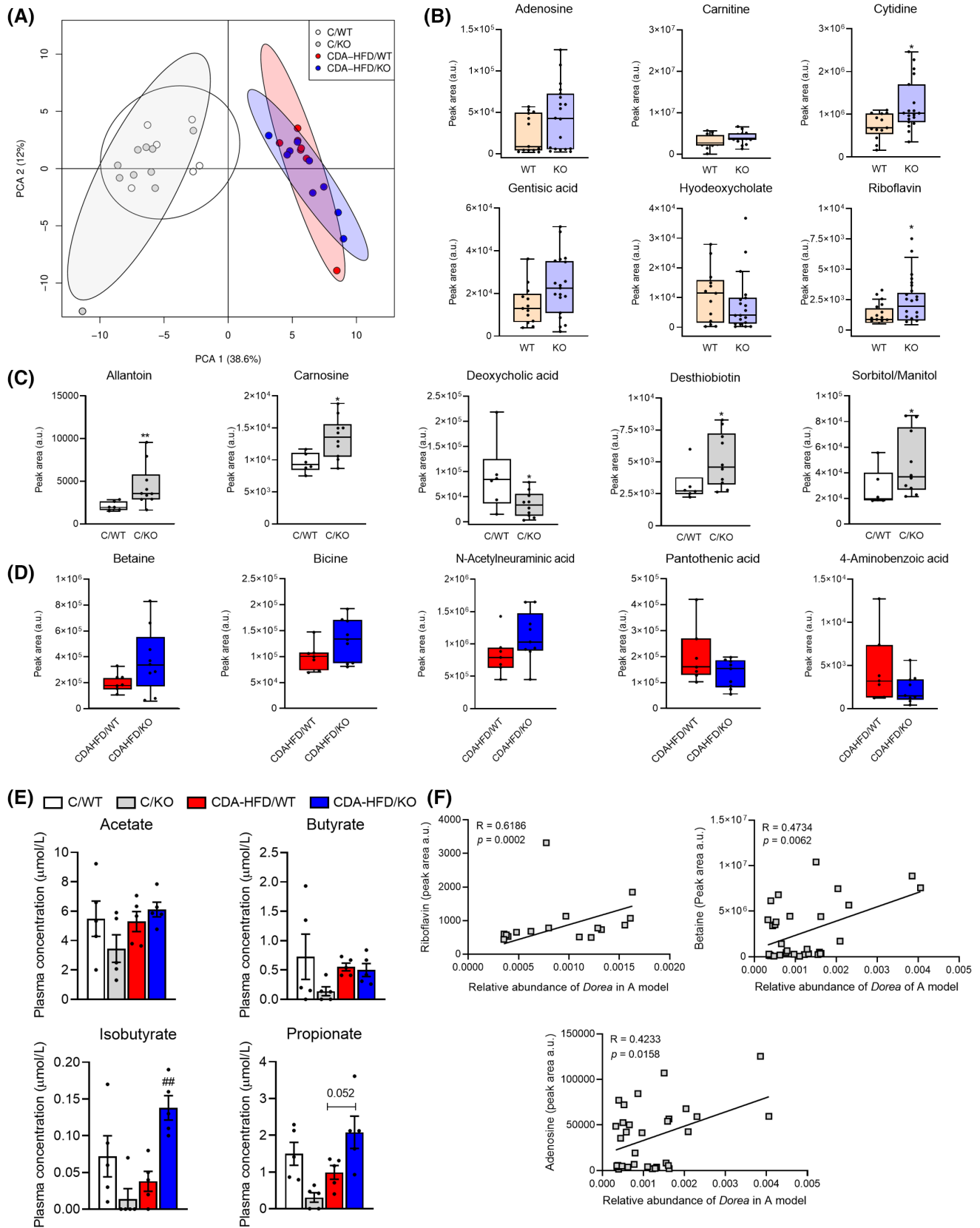


FIGURE 5 Fecal metabolomic analysis of A Model. (A) Principal component analysis of metabolite profiles. PC1 and PC2 values are shown in parentheses. Shaded areas denote sample clusters according to diet and genotype. (B) Differences in the metabolites between wild-type (WT) and methylation-controlled J protein knockout (MCJ-KO) mice independently of the diet. (C) Differences in the metabolites between WT and MCJ-KO mice fed with control diet. (D) Differences in the metabolites between WT and MCJ-KO mice fed with choline-deficient, L-amino acid–defined, high-fat diet (CDA-HFD). * $p < 0.05$. (E) Fecal concentration of the main short-chain fatty acids: acetate, butyrate, propionate, and isobutyrate. (F) Pearson's correlation coefficients, p values, and linear relationships of *Dorea* relative abundance and the peak area of adenosine, betaine, and riboflavin. At least $n = 5$ were used in each experimental group

whereas pantothenic acid and 4-aminobenzoic acid showed an opposite trend (Figure 5D).

In addition, the measurement of fecal short-chain fatty acids (SCFAs), one of the main metabolites related to gut microbiota functionality that are involved in the maintenance of gut barrier integrity, hepatic lipid metabolism, and inflammation,^[14] revealed that MCJ-KO mice significantly augmented their content with the diet, whereas CDA-HFD-fed WT mice showed reduced SCFAs when compared with control. Remarkably, CDA-HFD-fed MCJ-KO mice exhibited significantly increased propionate and isobutyrate concentrations compared with CDA-HFD-fed WT (Figure 5E).

Furthermore, a positive correlation was found between the relative abundance of *Dorea*, one of the main genera that characterizes the MCJ-KO gut microbiota signature, and the adenosine, betaine, and riboflavin levels, metabolites directly related to MCJ-KO genotype (Figure 5F).

To determine if the specific metabolomic profile associated with MCJ deficiency was also transferable through CMT to the B Model, the fecal metabolome of the transplanted GF mice was analyzed. The PCA showed that metabolites were clustered according to the diet based on the second axis (19.4%) but also a distribution caused by the gut microbiota was observed along the third axis (8.8%) related to the donor diet (Figure S7A). Furthermore, a second PCA was performed to identify the metabolome clustering in CDA-HFD, observing the effect of diet and genotype of the donors (Figure S7B). Additionally, adenosine, indole, isovalerylcarnitine, and riboflavin were partially increased in dC/KO recipients, resembling the profile observed in MCJ-KO mice (A Model) and suggesting a slight transferable effect through CMT (Figure S7C).

These results suggested that the specific metabolome related to MCJ deficiency observed in A Model was not completely transferred and maintained in GF mice, although some metabolite patterns, such as adenosine or riboflavin, were still detected in all GF mice groups and could be involved in the enhancement of NAD⁺ metabolism.

To confirm that increased hepatic NAD⁺ availability found in CDA-HFD-fed GF mice receiving MCJ-KO microbiota was due to a gut microbiome signature of MCJ deficiency, we measured expression of the main enzymes related to NAD⁺ metabolism and NAD⁺ levels in the gut. Interestingly, intestinal expression of *Nampt* and *Sirt1* was significantly increased in GF mice transplanted with MCJ-KO microbiota (Figure 6A) along with gut total NAD levels and the NAD⁺/NADH ratio (Figure 6B). Indeed, the dCDA-HFD/KO transplanted group exposed the highest intestinal NAD⁺/NADH ratio, confirming increased availability of NAD⁺. Intriguingly, a positive correlation between *Dorea* relative abundance and gut NAD total levels was observed (Figure 6C). Intestinal *Sirt1* expression was

also positively correlated with the relative abundance of *Dorea* genus (Figure 6D), similar to what happened with hepatic *Sirt1* levels. Besides, the same pattern was observed in the A Model with CDA-HFD-fed MCJ-KO mice (Figure 6E–G), suggesting a possible role of this bacteria in the NAD signaling pathway.

Altogether, our study shows that a specific microbiome signature derived from *Mcj*-deficient mice and its particular metabolism is able to delay NASH progression in a diet-induced NAFLD model and that this hepatoprotection is transferable through CMT.

Validation of the role of *Dorea* genus in a human cohort of patients with NAFLD

Additionally, *Dorea* stands out as one of the most relevant genera to understand the role of gut microbiota modulation in the protective effect against NAFLD development exerted by MCJ deficiency. This is not only due to its higher abundance in MCJ-KO mice and its complete transmission to GF mice but also because the correlation analysis pointed out that this genus is one of the main contributors of the observed effect. Therefore, we performed an analysis of publicly available human information to validate the relevance of this genus in human disease. Data from a cohort of twins and patients with cirrhosis^[15] was analyzed following the approach of Lee et al.^[16] Patients were divided according to their body mass index (BMI) into obese (BMI ≥ 30 ; $n = 71$) and non-obese (BMI < 30 ; $n = 121$), and interestingly, in the subset of nonobese subjects, the fecal abundance of *Dorea* was significantly lower with the presence of NAFLD ($p = 0.026$), whereas no significant differences were observed in patients with obesity ($p = 0.636$) (Figure S8). These findings could point to a specific change in gut microbiota composition in patients with lean NASH, characterized by a decrease of *Dorea* genus.

DISCUSSION

It is currently believed that 10%–20% of all subjects with NAFLD develop NASH, but the pathophysiology remains unclear.^[17] Mitochondrial dysfunction, oxidative stress, and gut microbiota alterations potentially play key roles in that transition.^[1] Recent data show that the lack of MCJ, an endogenous inhibitor of mitochondrial complex I, boosts mitochondrial activity in NASH.^[9] Moreover, the involvement of MCJ in the gut microbiota-host interplay during ulcerative colitis has been previously described.^[11] Therefore, we aimed to study the effect of increased mitochondrial activity in the gut-liver axis during NASH and to determine if the hepatoprotective phenotype observed in MCJ-KO mice might be microbiota-related and therefore transferred to GF mice recipients through CMT.

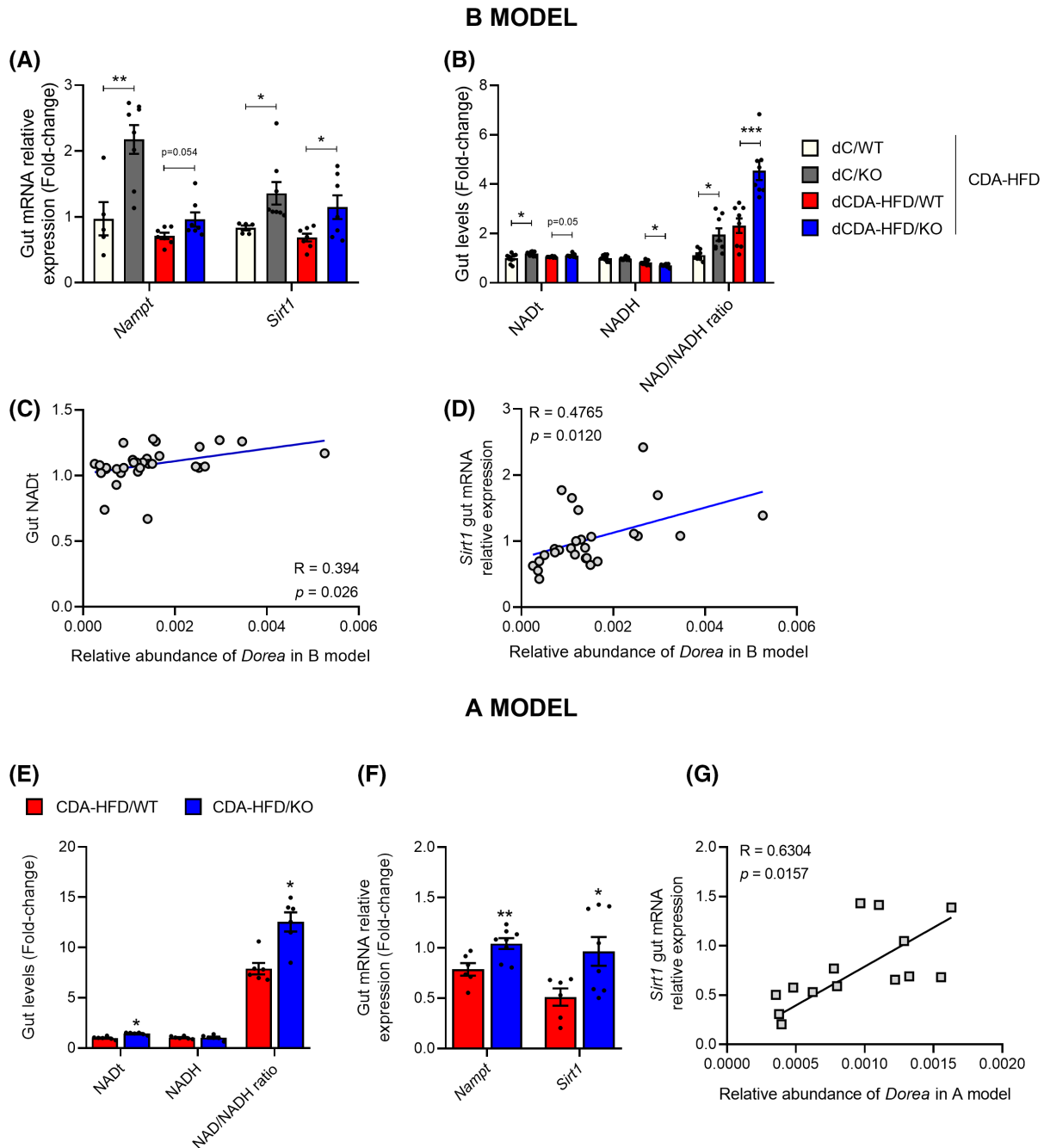


FIGURE 6 Intestinal nicotinamide adenine dinucleotide (NAD⁺) metabolism in both B and A Models. B Model, gut: (A) Relative messenger RNA (mRNA) expression of NAD⁺ synthesis enzymes nicotinamide phosphoribosyltransferase (*Nampt*) and *Sirtuin* (*Sirt*) 1. (B) Levels of total NAD (NADt), reduced nicotinamide adenine dinucleotide (NADH) and NAD⁺/NADH ratio. (C,D) Pearson's correlation coefficient, *p* value and linear relationship of the relative abundance of *Dorea* and (C) total NAD and (D) relative mRNA expression of *Sirt1* in animals fed with choline-deficient, L-amino acid–defined, high-fat diet (CDA-HFD) (blue line and dots). A Model, gut: (E) mRNA relative expression of NAD⁺ synthesis enzymes *Nampt* and *Sirt1*. (F) Levels of NADt, NADH, and NAD⁺/NADH ratio. At least *n* = 6 were used in each experimental group. **p* < 0.05; ***p* < 0.01, ****p* < 0.001 versus CDA-HFD/wild type (WT). (G) Pearson's correlation coefficient, *p* value, and linear relationship of the relative abundance of *Dorea* and the relative mRNA expression of *Sirt1* in animals fed with CDA-HFD (black line and squares)

In line with our previous findings,^[9] lack of MCJ after CDA-HFD for 6 weeks counteracted inflammation and fibrosis, reinforcing the potential protective effect of MCJ deficiency in NAFLD development. Although the role of the gut-liver axis in NASH progression has been profoundly reported,^[2] the effects of MCJ-KO in the gut

status and gut microbiota composition had not been investigated. In our study, under steatotic conditions, MCJ deficiency increased expression of the main tight junction proteins and decreased endotoxin (Lipid A) and proinflammatory cytokines levels in plasma. Interestingly, MCJ-KO mice showed improved gut-liver

axis status with downregulated hepatic *Tlr-4* and *Nlrp3*, sensors of potential gut microbiota-derived hepatotoxic or immunostimulatory compounds.^[18] Therefore, an improved mitochondrial activity, caused by MCJ deficiency, counteracted the altered gut-liver axis that characterizes NAFLD progression because it reinforced the gut barrier and diminished the translocation of bacterial product to the portal blood circulation that aggravates liver inflammation and accelerates disease progression.^[19]

Furthermore, MCJ-KO mice exhibited a specific gut microbiota composition independently of the diet, characterized by an increase in *Dorea* genus and a reduction in *AF12*, *Allobaculum*, and [*Ruminococcus*]. In these terms, some studies have shown the implication of *Dorea* genus in NAFLD.^[3,20] However, in both cases, research was focused on subjects with obesity, and a positive correlation between *Dorea* and BMI was demonstrated. Therefore, the decrease in this genus might be attributed to the metabolic status instead of liver disease.^[21,22] In fact, the analysis of a public cohort of patients with NAFLD showed that *Dorea* is significantly decreased in patients with NAFLD who are nonobese compared with those with no NAFLD. Additionally, CDA-HFD has been reported as an aggressive dietary model of lean NASH, producing an advanced status of the disease without promoting obesity.^[12] Thus, in our study, the increase in *Dorea* genus in CDA-HFD/KO mice could be involved in the observed protective effect. Besides, the abundance of *Dorea* has been reported to increase after a treatment with a multistrain probiotic, associated with the reduction of the hepatic fat fraction.^[23] Additionally, *Allobaculum* was associated with high-fat diet-feeding in NAFLD mice models,^[13,24] and *Ruminococcus* abundance has been widely related to NAFLD development,^[3,20] reinforcing our results. However, it is noteworthy that, in our study, the particular microenvironment and the consequent specific metabolism caused by the genotype could certainly be shaping the gut microbiota^[25] in an MCJ-KO-dependent way, resulting in a microbiota signature.

Related to the specific microbiome signature in MCJ-KO mice, fecal metabolome analysis showed an increase in adenosine, cytidine, or riboflavin independently of the diet, whereas other metabolites, such as betaine, tended to increase in CDA-HFD-fed MCJ-KO mice. Enhanced mitochondrial activity might be the reason for the high levels of both adenosine^[26] and betaine.^[27,28] Adenosine exerts anti-inflammatory effects and is implicated in the control of intestinal barrier function.^[26] Besides, different studies have demonstrated the antioxidant properties and the beneficial role of betaine in NAFLD development because of its ability to scavenge ROS, protect mitochondria complex II, and regenerate mitochondrial glutathione levels.^[27,28] Betaine also improves small intestine status

and intestinal permeability as well as consolidates the tight junctions in acute liver failure, shaping the gut microbiota composition in mice.^[29] Interestingly, significantly increased fecal concentrations of propionate and isobutyrate were found in CDA-HFD-fed MCJ-KO mice, two of the main SCFAs linked to beneficial effects on human health. Indeed, treatment with SCFAs has shown antioxidant effects, downregulation of proinflammatory mediators, maintenance of gut barrier integrity, and increased mitochondrial respiratory capacity.^[14,30,31]

Importantly, our analysis showed a positive correlation between adenosine and betaine and the abundance of *Dorea* genus, one of the main taxa associated with MCJ-KO genotype, suggesting the regulation of *Dorea* abundance by these metabolites, as has previously been shown.^[32,33] In summary, the abundance of these metabolites could be determining an MCJ-KO specific microbial signature, mainly increasing the gut fitness of *Dorea* genus species.

The CMT from MCJ-KO mice to CDA-HFD-fed GF mice ameliorated the hepatic injury and induced a partial restoration of gut barrier integrity and gut-liver axis status, demonstrating that the protective effect of the genotype is transmissible by the microbiota. Previous experiments in GF mice have proved that the inflammatory status may be transmissible through the microbiota and that the adaptations induced by a genetic variant may have an impact on gut microbiota susceptible to being replicated in gnotobiotic recipients.^[34–36] Moreover, the same patterns observed in A Model on the relative abundance of *AF12*, *Dorea*, *Oscillospira*, and [*Ruminococcus*] were detected in B Model, corroborating that the hepatoprotective effect was mediated by this specific microbiome signature.

We next tried to understand how this bacterial community, shaped by the MCJ-KO-dependent metabolome, could have protective effects both in the gut and in the liver following a dietary NASH model. We have already described how the lack of MCJ increases the mitochondrial activity and ATP production,^[8] affecting NAD metabolism. A significantly increased NAD⁺/NADH ratio was observed in MCJ-KO mice, both in liver and intestinal tissues, and, interestingly, also in CDA-HFD-fed GF mice after CMT from MCJ-KO genotype. NAD⁺ not only plays a key role in energy metabolism and fueling mitochondrial function but is also a precursor for NADPH, an important component of the antioxidant defense system.^[37] In fact, NAD⁺ has been proposed as a potential target to prevent and reverse NAFLD.^[38] NAD⁺ precursors have been found to improve hepatic mitochondrial function and decrease oxidative stress in preclinical models of NAFLD,^[39] and its repletion also prevents progression to NASH.^[40] In line with these findings, CDA-HFD-fed MCJ-KO (A Model) and GF mice (B Model) showed improved mitochondrial function and higher lipid beta oxidation activity in their livers. Additionally, the contribution of

gut microbiota in NAD⁺ biosynthesis and regulation has been slightly described.^[41] In our study, the increased levels of NAD⁺ observed in the liver and the gut were associated with a higher abundance of *Dorea* genus not only in MCJ-KO mice but also in GF mice. Based on previous studies, we hypothesize that increased levels of SCFAs found in CDA-HFD-fed MCJ-KO mice might be enhancing intestinal metabolism and thus enabling the augmented NAD⁺ levels.^[30] Overall, these data point out a possible mechanism underlying the protective effect of MCJ-KO gut microbiota during NASH development.

Additionally, NAD⁺ also serves as a substrate for a wide range of enzymes, including SIRT.^[38] Hepatic SIRT1 activity reduces *de novo* lipogenesis and enhances beta oxidation,^[42] and in the gut, SIRT1 exerts anti-inflammatory effects in acute intestinal inflammation,^[43] maintaining gut barrier function.^[44] We observed significantly higher hepatic and gut mRNA levels of *Sirt1* in CDA-HFD-fed MCJ-KO (A Model) as well as in GF mice transplanted with MCJ-KO microbiota and fed with CDA-HFD (B Model). In fact, as in the case of the NAD⁺/NADH ratio, positive correlations were observed, both in liver and gut tissues, between *Sirt1* expression and *Dorea* abundance in the two models. Hydrogen is capable of avoiding downregulation of sirtuins as well as restoring mitochondrial NAD⁺ production,^[45] and *Dorea* is a hydrogen-producer genus.^[46] Thus, the abundance of *Dorea* observed in our study could be promoting an augment of hydrogen levels and, consequently, an enhancement in SIRT1 activity and NAD⁺ biosynthesis, mediating the protective effect in NAFLD development.

Currently, there is not an efficient approved therapy to halt or reverse lean NASH. Considering its increasing prevalence along with the severity of patients with lean NASH, therapeutic alternatives are strictly required. Herein, MCJ deficiency and the consequently improved mitochondrial activity reshape a specific and protective microbiome signature able to delay the disease progression in an aggressive NASH-lean dietary model. Overall, these results highlight the importance of mitochondria-microbiota crosstalk in NASH and point to therapeutic strategies based on microbiota transplantation, paving the way for different approaches.

AUTHOR CONTRIBUTIONS

Conception or design of the work: María Juárez-Fernández, Naroa Goikoetxea-Usandizaga, María Luz Martínez-Chantar, Sonia Sánchez-Campos. Acquisition, analysis, or interpretation of data: María Juárez-Fernández, Naroa Goikoetxea-Usandizaga, David Porras, María Victoria Garcia-Mediavilla, Héctor Rodríguez, Esther Nistal, Miren Bravo, Marina Serrano-Maciá, Jorge Simón, Teresa C. Delgado, Sofía Lachiondo-Ortega, Susana Martínez-Flórez, Óscar Lorenzo, Mercedes Rincón, Marta Varela-Rey, Leticia Abecia, Juan Anguita, María Luz Martínez-Chantar,

Sonia Sánchez-Campos. Drafted the work: María Juárez-Fernández, Naroa Goikoetxea-Usandizaga, María Luz Martínez-Chantar, Sonia Sánchez-Campos. Substantively revised the work: María Juárez-Fernández, Naroa Goikoetxea-Usandizaga, Esther Nistal, María Luz Martínez-Chantar, Sonia Sánchez-Campos.

FUNDING INFORMATION

This work was supported by grants from Ministerio de Ciencia e Innovación, Programa Retos-Colaboración RTC2019-007125-1 (for Jorge Simón and María Luz Martínez-Chantar); Instituto de Salud Carlos III, Proyectos de Investigación en Salud DTS20/00138 (for Jorge Simón and María Luz Martínez-Chantar); Departamento de Industria del Gobierno Vasco (for María Luz Martínez-Chantar); Ministerio de Ciencia, Innovación y Universidades MICINN: PID2020-117116RB-I00 integrado en el Plan Estatal de Investigación Científica y Técnica y de Innovación, cofinanciado con Fondos FEDER (for María Luz Martínez-Chantar); Ayudas Ramón y Cajal de la Agencia Estatal de Investigación RY2013-13666 (for Leticia Abecia); BIOEF (Basque Foundation for Innovation and Health Research); Asociación Española contra el Cáncer (for María Luz Martínez-Chantar); Fundación Científica de la Asociación Española Contra el Cáncer (AECC Scientific Foundation) Rare Tumor Calls 2017 (for María Luz Martínez-Chantar); La Caixa Foundation Program (for María Luz Martínez-Chantar); Proyecto Desarrollo Tecnológico CIBERehd (for María Luz Martínez-Chantar). This work was also supported by grants from Ministerio de Economía y Competitividad/FEDER (BFU2017-87960-R; PID2020-120363RB-I0) (for Sonia Sánchez-Campos) and Junta de Castilla y León (FEDER) (GRS2126/A/2020; LE063U16; LE017P20) (for J.G.-G and Sonia Sánchez-Campos). María Juárez-Fernández was supported by a fellowship from Ministerio de Ciencia, Innovación y Universidades (FPU18/06257) and David Porras by a fellowship from Junta de Castilla y León cofunded by the European Social Fund. CIBERehd is funded by the Instituto de Salud Carlos III, Spain. The authors want to thank Dr. Danielsen from MS-Omics for performing the metabolomic analysis and Unidad de Genómica of SCSIE from Universitat de Valencia for metagenomic analysis.

CONFLICTS OF INTEREST

Dr. Rincón is the Scientific Founder of Mitotherapeutix LLC, and Dr. Martínez-Chantar advises Mitotherapeutix LLC.

DATA AVAILABILITY STATEMENT

Data are available upon reasonable request. The 16S sequencing data of this study have been deposited in the European Nucleotide Archive (ENA) at EMBL-EBI under accession number PRJEB55379.

ORCID

María Juárez-Fernández  <https://orcid.org/0000-0003-4678-3058>
 Naroa Goikoetxea-Usandizaga  <https://orcid.org/0000-0003-4569-028X>
 David Porras  <https://orcid.org/0000-0002-8824-7504>
 María Victoria García-Mediavilla  <https://orcid.org/0000-0002-5722-7500>
 Miren Bravo  <https://orcid.org/0000-0001-5889-9125>
 Marina Serrano-Maciá  <https://orcid.org/0000-0003-4183-6384>
 Jorge Simón  <https://orcid.org/0000-0003-0404-6244>
 Teresa C. Delgado  <https://orcid.org/0000-0001-9204-581X>
 Sofía Lachiondo-Ortega  <https://orcid.org/0000-0003-1856-3664>
 Susana Martínez-Flórez  <https://orcid.org/0000-0002-7200-8744>
 Óscar Lorenzo  <https://orcid.org/0000-0001-5515-6078>
 Leticia Abecía  <https://orcid.org/0000-0003-4097-8903>
 Héctor Rodríguez  <https://orcid.org/0000-0002-9948-2497>
 Juan Anguita  <https://orcid.org/0000-0003-2061-7182>
 Esther Nistal  <https://orcid.org/0000-0002-2201-5575>
 María Luz Martínez-Chantar  <https://orcid.org/0000-0002-6446-9911>
 Sonia Sánchez-Campos  <https://orcid.org/0000-0003-2672-734X>

REFERENCES

- Ballard JWO, Towarnicki SG. Mitochondria, the gut microbiome and ROS. *Cell Signal*. 2020;75:109737.
- Ye JZ, Li YT, Wu WR, Shi D, Fang DQ, Yang LY, et al. Dynamic alterations in the gut microbiota and metabolome during the development of methionine-choline-deficient diet-induced nonalcoholic steatohepatitis. *World J Gastroenterol*. 2018;24:2468–81.
- Boursier J, Mueller O, Barret M, Machado M, Fizanne L, Araujo-Perez F, et al. The severity of nonalcoholic fatty liver disease is associated with gut dysbiosis and shift in the metabolic function of the gut microbiota. *Hepatology*. 2016;63:764–75.
- Clark A, Mach N. The crosstalk between the gut microbiota and mitochondria during exercise. *Front Physiol*. 2017;8:319.
- Saint-Georges-Chaumet Y, Edeas M. Microbiota-mitochondria inter-talk: consequence for microbiota-host interaction. *Pathog Dis*. 2016;74:ftv096.
- Hatle KM, Gummadijala P, Navasa N, Bernardo E, Dodge J, Silverstrim B, et al. MCJ/DnaJC15, an endogenous mitochondrial repressor of the respiratory chain that controls metabolic alterations. *Mol Cell Biol*. 2013;33:2302–14.
- Navasa N, Martín I, Iglesias-Pedraz JM, Beraza N, Atondo E, Izadi H, et al. Regulation of oxidative stress by methylation-controlled J protein controls macrophage responses to inflammatory insults. *J Infect Dis*. 2015;211:135–45.
- Barbier-Torres L, Iruzubieta P, Fernández-Ramos D, Delgado TC, Taibo D, Guitierrez-de-Juan V, et al. The mitochondrial negative regulator MCJ is a therapeutic target for acetaminophen-induced liver injury. *Nat Commun*. 2017;8:2068.
- Barbier-Torres L, Fortner KA, Iruzubieta P, Delgado TC, Giddings E, Chen Y, et al. Silencing hepatic MCJ attenuates non-alcoholic fatty liver disease (NAFLD) by increasing mitochondrial fatty acid oxidation. *Nat Commun*. 2020;11:3360.
- Iruzubieta P, Goikoetxea-Usandizaga N, Barbier-Torres L, Serrano-Maciá M, Fernández-Ramos D, Fernández-Tussy P, et al. Boosting mitochondria activity by silencing MCJ overcomes cholestasis-induced liver injury. *JHEP Rep*. 2021;3:100276.
- Pascual-Itoiz MA, Peña-Cearra A, Martín-Ruiz I, Lavín JL, Simó C, Rodríguez H, et al. The mitochondrial negative regulator MCJ modulates the interplay between microbiota and the host during ulcerative colitis. *Sci Rep*. 2020;10:572.
- Matsumoto M, Hada N, Sakamaki Y, Uno A, Shiga T, Tanaka C, et al. An improved mouse model that rapidly develops fibrosis in non-alcoholic steatohepatitis. *Int J Exp Pathol*. 2013;94:93–103.
- Le Roy T, Llopis M, Lepage P, Bruneau A, Rabot S, Bevilacqua C, et al. Intestinal microbiota determines development of non-alcoholic fatty liver disease in mice. *Gut*. 2013;62:1787–94.
- Fairfield B, Schnabl B. Gut dysbiosis as a driver in alcohol-induced liver injury. *JHEP Rep*. 2020;3:100220.
- Caussy C, Hsu C, Singh S, Bassirian S, Kolar J, Faulkner C, et al. Serum bile acid patterns are associated with the presence of NAFLD in twins, and dose-dependent changes with increase in fibrosis stage in patients with biopsy-proven NAFLD. *Aliment Pharmacol Ther*. 2019;49:183–93.
- Lee G, You HJ, Bajaj JS, Joo SK, Yu J, Park S, et al. Distinct signatures of gut microbiome and metabolites associated with significant fibrosis in non-obese NAFLD. *Nat Commun*. 2020;11(1):4982.
- Pierantonelli I, Svegliati-Baroni G. Nonalcoholic fatty liver disease: basic pathogenetic mechanisms in the progression from NAFLD to NASH. *Transplantation*. 2019;103:E1–E13.
- Meli R, Raso GM, Calignano A. Role of innate immune response in non-alcoholic fatty liver disease: metabolic complications and therapeutic tools. *Front Immunol*. 2014;5:177.
- Hu H, Lin A, Kong M, Yao X, Yin M, Xia H, et al. Intestinal microbiome and NAFLD: molecular insights and therapeutic perspectives. *J Gastroenterol*. 2020;55:142–58.
- Velázquez KT, Enos RT, Bader JE, Sougiannis AT, Carson MS, Chatzistamou I, et al. Prolonged high-fat-diet feeding promotes non-alcoholic fatty liver disease and alters gut microbiota in mice. *World J Hepatol*. 2019;11:619–37.
- Gallè F, Valeriani F, Cattaruzza MS, Gianfranceschi G, Liguori R, Antinozzi M, et al. Mediterranean diet, physical activity and gut microbiome composition: a cross-sectional study among healthy young Italian adults. *Nutrients*. 2020;12:2164.
- Jiao N, Baker SS, Nugent CA, Tsompana M, Cai L, Wang Y, et al. Gut microbiome may contribute to insulin resistance and systemic inflammation in obese rodents: a meta-analysis. *Physiol Genomics*. 2018;50:244–54.
- Ahn SB, Jun DW, Kang BK, Lim JH, Lim S, Chung MJ. Randomized, double-blind, placebo-controlled study of a multi-species probiotic mixture in nonalcoholic fatty liver disease. *Sci Rep*. 2019;9:5688.
- Safari Z, Monnoye M, Abuja PM, Mariadassou M, Kashofer K, Gérard P, et al. Steatosis and gut microbiota dysbiosis induced by high-fat diet are reversed by 1-week chow diet administration. *Nutr Res*. 2019;71:72–88.
- Gomaa EZ. Human gut microbiota/microbiome in health and diseases: a review. *Antonie van Leeuwenhoek*. 2020;113:2019–40.
- D'Antongiovanni V, Fornai M, Pellegrini C, Benevenuti L, Blandizzi C, Antonioli L. The adenosine system at the crossroads of intestinal inflammation and neoplasia. *Int J Mol Sci*. 2020;21:5089.
- Khodayar MJ, Kalantari H, Khorsandi L, Rashno M, Zeidooni L. Betaine protects mice against acetaminophen hepatotoxicity possibly via mitochondrial complex II and glutathione availability. *Biomed Pharmacother*. 2018;103:1436–45.

28. Zhang L, Qi Y, ALuo Z, Liu S, Zhang Z, Zhou L. Betaine increases mitochondrial content and improves hepatic lipid metabolism. *Food Funct.* 2019;10:216–23.
29. Chen Q, Wang Y, Jiao F, Shi C, Pei M, Wang L, et al. Betaine inhibits Toll-like receptor 4 responses and restores intestinal microbiota in acute liver failure mice. *Sci Rep.* 2020;10:21850.
30. González-Bosch C, Boorman E, Zunszain PA, Mann GE. Short-chain fatty acids as modulators of redox signaling in health and disease. *Redox Biol.* 2021;47:102165.
31. Leung C, Rivera L, Furness JB, Angus PW. The role of the gut microbiota in NAFLD. *Nat Rev Gastroenterol Hepatol.* 2016;13:412–25.
32. Liu Y, Du T, Zhang W, Lu W, Peng Z, Huang S, et al. Modified Huang-Lian-Jie-Du Decoction ameliorates A β synaptotoxicity in a murine model of Alzheimer's disease. *Oxid Med Cell Longev.* 2019;2019:8340192.
33. Du J, Zhang P, Luo J, Shen L, Zhang S, Gu H, et al. Dietary betaine prevents obesity through gut microbiota-driven microRNA-378a family. *Gut Microbes.* 2021;13:1862612.
34. Liao L, Schneider KM, Galvez EJC, Frissen M, Marschall HU, Su H, et al. Intestinal dysbiosis augments liver disease progression via NLRP3 in a murine model of primary sclerosing cholangitis. *Gut.* 2019;68:1477–92.
35. Soderborg TK, Clark SE, Mulligan CE, Janssen RC, Babcock L, Ir D, et al. The gut microbiota in infants of obese mothers increases inflammation and susceptibility to NAFLD. *Nat Commun.* 2018;9:4462.
36. Wen L, Ley RE, Volchkov PY, Stranges PB, Avanesyan L, Stonebraker AC, et al. Innate immunity and intestinal microbiota in the development of Type 1 diabetes. *Nature.* 2008;455:1109–13.
37. Katsyuba E, Mottis A, Zietak M, de Franco F, van der Velpen V, Gariani K, et al. De novo NAD⁺ synthesis enhances mitochondrial function and improves health. *Nature.* 2018;563:354–9.
38. Dall M, Hassing AS, Treebak JT. NAD⁺ and NAFLD—caution, causality and careful optimism. *J Physiol.* 2021;600:1135–54.
39. Ganji SH, Kukes GD, Lambrecht N, Kashyap ML, Kamanna VS. Therapeutic role of niacin in the prevention and regression of hepatic steatosis in rat model of nonalcoholic fatty liver disease. *Am J Physiol Gastrointest Liver Physiol.* 2014;306:G320–7.
40. Dall M, Hassing AS, Niu L, Nielsen TS, Ingerslev LR, Sulek K, et al. Hepatocyte-specific perturbation of NAD⁺ biosynthetic pathways in mice induces reversible nonalcoholic steatohepatitis-like phenotypes. *J Biol Chem.* 2021;297:101388.
41. Shats I, Williams JG, Liu J, Makarov MV, Wu X, Lih FB, et al. Bacteria boost mammalian host NAD metabolism by engaging the deamidated biosynthesis pathway. *Cell Metab.* 2020;31:564–79.e7.
42. Li Y, Wong K, Giles A, Jiang J, Lee JW, Adams AC, et al. Hepatic SIRT1 attenuates hepatic steatosis and controls energy balance in mice by inducing fibroblast growth factor 21. *Gastroenterology.* 2014;146:539–49.e7.
43. Lakhani SE, Kirchgessner A. Gut microbiota and sirtuins in obesity-related inflammation and bowel dysfunction. *J Transl Med.* 2011;9:202.
44. Ren MT, Gu ML, Zhou XX, Yu MS, Pan HH, Ji F, et al. Sirtuin 1 alleviates endoplasmic reticulum stress-mediated apoptosis of intestinal epithelial cells in ulcerative colitis. *World J Gastroenterol.* 2019;25:5800–13.
45. Niu Y, Nie Q, Dong L, Zhang J, Liu SF, Song W, et al. Hydrogen attenuates allergic inflammation by reversing energy metabolic pathway switch. *Sci Rep.* 2020;10:1962.
46. Shen J, Ding Y, Yang Z, Zhang X, Zhao M. Effects of changes on gut microbiota in children with acute Kawasaki disease. *PeerJ.* 2020;8:e9698.

SUPPORTING INFORMATION

Additional supporting information can be found online in the Supporting Information section at the end of this article.

How to cite this article: Juárez-Fernández M, Goikoetxea-Usandizaga N, Porrás D, García-Mediavilla MV, Bravo M & Serrano-Maciá M et al. Enhanced mitochondrial activity reshapes a gut microbiota profile that delays NASH progression. *Hepatology.* 2022;00:1–16. <https://doi.org/10.1002/hep.32705>